Estimation of absorption and backscattering coefficients from in situ radiometric measurements: theory and validation in case II waters

David McKee, Alex Cunningham, and Susanne Craig

A model that relates the coefficients of absorption (a) and backscattering (b_b) to diffuse attenuation (K_d), radiance reflectance (R_L), and the mean cosine for downward irradiance (μ_d) is presented. Radiance transfer simulations are used to verify the physical validity of the model for a wide range of water column conditions. Analysis of these radiance transfer simulations suggests that absorption and backscattering can be estimated with average errors of 1% and 3%, respectively, if the value of μ_d is known with depth. If the input data set is restricted to variables that can be derived from measurements of upward radiance (L_u) and downward irradiance (E_d), it is necessary to use approximate values of μ_d. Examination of three different approximation schemes for μ_d shows that the average error for estimating a and b_b increases to ~13%. We tested the model by using measurements of L_u and E_d collected from case II waters off the west coast of Scotland. The resulting estimates of a and b_b were compared with independent *in situ* measurements of these parameters. Average errors for the data set were of the order of 10% for both absorption and backscattering.

OCIS codes: 010.4450, 290.1350, 300.1030.

1. Introduction

Interest in the relationship between inherent optical properties (IOPs) and apparent optical properties (AOPs) stems largely from the need for improved quantitative interpretation of remote-sensing images. The ultimate goal is the production of maps of biomass and primary productivity, but the recovery of IOPs would be a useful intermediate step as total IOPs can be partitioned into components that are directly related to seawater constituents. A second application of this type of analysis is to test the mutual consistency of concurrent *in situ* measurements of IOPs and AOPs, which requires simple, reliable relationships that can be quickly applied to large data sets. Moreover, hyperspectral profiling radiometers are now readily available, and a reliable method of estimating IOPs from AOPs would provide new insight into the spectral variability of absorption and backscattering coefficients that are currently difficult to measure directly.

There has been considerable activity in this area in recent years. Lee *et al.*[1] produced a method for deriving absorption coefficients from radiance reflectance (R_L) measurements, whereas Leathers and McCormick[2] and Leathers *et al.*[3] developed methods of estimating absorption and backscattering that use measurements of R_L and irradiance reflectance (R). All these retrieval techniques are based on assumptions that concern the scattering phase function ($\tilde{\beta}$). Further efforts have been made to derive relationships that avoid making assumptions with regard to $\tilde{\beta}$[4], and the effect of Raman scattering on this type of relationship has been examined.[5] Here we derive a simple relationship between IOPs and AOPs that neglects inelastic processes and makes no assumptions with regard to the shape of $\tilde{\beta}$. The derived relationship enables estimation of both absorption and backscattering coefficients from measurements of the diffuse attenuation coefficient (K_d), radiance reflectance (R_L), and mean cosine for downward irradiance (μ_d).

One reason for deriving this model was to devise a method for estimating IOPs solely from measurements of downward irradiance E_d and upward radiance L_u. These are the parameters measured by the most common configuration for *in situ* radiometer

The authors are with the Department of Physics and Applied Physics, University of Strathclyde, 107 Rottenrow, Glasgow, Scotland G4 0NG, United Kingdom. The e-mail address for D. McKee is david.mckee@strath.ac.uk.

Received 9 September 2002; Revised manuscript received 28 January 2003.

0003-6935/03/152804-07$15.00/0

systems, particularly for remote-sensing applications. Such a limited set of input data eliminates the use of several models that require additional information such as upward irradiance (E_u). Two of the AOPs required for the model derived in this paper (K_d and R_L) can be obtained from *in situ* measurements of downward irradiance (E_d) and upward radiance (L_u). One limitation of this method at present, however, is the need to use an approximate value for the mean cosine for downward irradiance (μ_d). Various strategies for estimation of μ_d are discussed and the errors associated with each are examined. A second limitation is that the current analysis is restricted to wavelengths between 400 and 560 nm, where inelastic scattering processes make only a minor contribution in surface waters. Radiative transfer models are used to assess the validity of the model for a range of solar elevations, scattering phase functions, and water column composition. The effects of a diffuse sky and inhomogeneous water column structure are also simulated. Primary validation of the model is achieved by use of field data collected in case II waters off the west coast of Scotland.

2. Theory

A. Model Derivation

Gordon[6] used a series of Monte Carlo simulations to demonstrate that the diffuse attenuation coefficient could be related to absorption and backscattering by

$$K_d = \frac{g(a + b_b)}{\mu_d}, \tag{1}$$

where μ_d is the average cosine for downward irradiance and g is a constant whose value was determined by linear regression. This relationship appeared to be independent of the scattering phase function used to generate it in the Monte Carlo simulations. For Gordon's modeling conditions g was found to have a value of 1.0395.

Morel and Gentili[7] showed that radiance reflectance R_L could be related to absorption a and backscattering b_b by

$$R_L = \frac{f}{Q}\frac{b_b}{a}, \tag{2}$$

where Q is the ratio of upward irradiance to radiance (E_u/L_u) and f is a factor that varies with solar angle and with the optical properties of the water column. The ratio of f/Q in Eq. (2) was shown to be fairly insensitive to solar angle, and in the blue-green part of the spectrum f/Q was shown to lie within a reasonably narrow range ($\sim$0.09–0.11) with an average value of 0.0936.

Equations (1) and (2) were derived independently from different underlying assumptions, but if they are taken at face value they can be rearranged to give

$$a = \frac{K_d\mu_d}{g\left[1 + \dfrac{R_L}{f/Q}\right]}, \tag{3}$$

$$b_b = \frac{K_d\mu_d}{g\left[1 + \dfrac{f/Q}{R_L}\right]}. \tag{4}$$

Equations (3) and (4) give two IOPs (a and b_b) in terms of the diffuse attenuation coefficient K_d, the radiance reflectance R_L, and the mean cosine of downward irradiance μ_d.

One apparent difficulty is that Eqs. (1) and (2) were derived for surface values of K_d and R_L. To determine if Eqs. (3) and (4) are applicable to depths greater than zero, the validity of Eq. (1) and (2) as a function of depth will be examined by use of the results of radiance transfer simulations. These simulations can also be used to establish whether Eqs. (3) and (4) are physically realistic. It should be noted that Eq. (3) is of the same form as Eq. (16) from Lee *et al.*,[1] though they used $K_{d,av}$, the average diffuse attenuation coefficient in the euphotic zone.

B. Further Considerations

One of the aims of this paper is to derive a relationship between AOPs and IOPs that uses the information produced by the E_d–L_u radiometer configuration. K_d and R_L can be derived from profiles of downward irradiance E_d and upward radiance L_u. Unfortunately there does not appear to be a simple manner in which the mean cosine μ_d can be obtained as a function of depth from E_d and L_u measurements. A number of potential approximations are available however. The simplest approximation would be to adopt a mean value of the mean cosine for all conditions. For example, if it is assumed that the mean cosine varies between 0.5 and 1, then a mean value of 0.75 could be adopted. Alternatively, Gordon[6] provided modeled values of the variation in mean cosine just beneath the sea surface for changes in solar zenith angle at three wavelengths in the blue-green part of the spectrum. Figure 1 shows this data plotted as $\mu_d(0)$ versus $\cos(\theta_{sw})$ for solar zenith angles up to 60°. A linear fit to the data provides

$$\mu_d(0) = 0.827\ \cos(\theta_{sw}) + 0.144, \tag{5}$$

where θ_{sw} is the solar zenith angle measured beneath the sea surface. Equation (5) can be used to estimate the mean cosine for downward irradiance just beneath the surface for wavelengths in the blue-green part of the spectrum and for solar zenith angles between 0° and 60°. The solar zenith angle underwater, θ_{sw}, can be obtained from the in-air solar zenith angle θ_a by use of Snell's law:

$$\theta_{sw} = \sin^{-1}\left(\frac{\sin\theta_a}{n_w}\right), \tag{6}$$

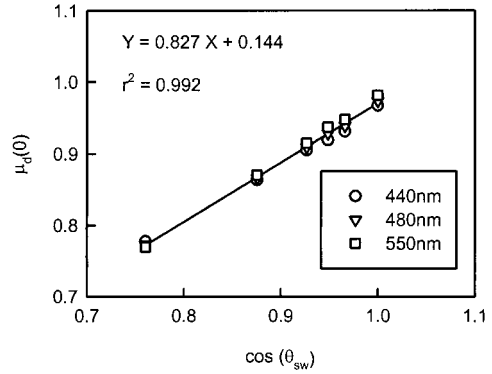

Fig. 1. Linear relationship between the cosine of the solar zenith angle measured underwater and the mean cosine for downward irradiance immediately beneath the sea surface. Data from Table 3 in Ref. 6.

where n_w is the refractive index of seawater ($\approx$1.34). One option for estimating the mean cosine is, therefore, to assume that $\mu_d(z) \approx \mu_d(0)$ and to use Eqs. (5) and (6) to derive $\mu_d(0)$.

Another interesting conclusion in the Gordon[6] paper is that the product $K_d\mu_d$ behaves like an IOP. If Eq. (1) is valid for depths greater than zero, for homogeneous waters the product $K_d\mu_d$ should be constant with depth. Thus for a homogeneous water column, if $\mu_d(0)$ is derived from the solar zenith angle by use of Eq. (5) and $K_d(0)$ is known, the numerator of Eqs. (3) and (4) can be replaced by the product of $K_d(0)\ \mu_d(0)$.

Three approximations have been identified: $K_d(z)\mu_d(z) = K_d(z)0.75$, $K_d(z)\mu_d(z) = K_d(z)\mu_d(0)$, and $K_d(z)\mu_d(z) = K_d(0)\mu_d(0)$. The use of approximations for $K_d(z)\mu_d(z)$ would undoubtedly introduce additional errors into the estimation of a and b_b. The effect of each approximation can be examined by application of the model to the results of radiance transfer simulations carried out for a wide range of input conditions. This analysis should provide guidance as to which approximation to adopt when the model is applied to field data.

3. Materials and Methods

A. Radiometric Measurements and Apparent Optical Property Derivation

Downward irradiance (E_d) and upward radiance (L_u) were measured in seven wavebands (10-nm FWHM) across the visible spectrum by use of a Satlantic Sea WiFS (Sea-viewing Wide Field-of-view Sensor) Profiling Multichannel Radiometer (SPMR). The SPMR was deployed at a distance of at least 20 m from the ship to avoid shadowing. The stability of the SPMR and deck reference irradiance sensors was monitored at the start and at the end of the cruise by use of a 100-W standard lamp, and the SPMR radiance sensors were checked with the same lamp illuminating a Spectralon reflectance target. All the sensors remained within factory specifications. Signals from the SPMR were processed with ProSoft, a Matlab module supplied by the manufacturers. Data processing steps included the application of calibration constants, averaging over 1-m depth intervals, and deriving diffuse attenuation coefficients (K_d) and radiance reflectances ($R_L = L_u/E_d$).

B. Inherent Optical Property Measurements

A 25-cm path-length Wet Labs ac-9 was used to measure the absorption coefficient (a) and beam attenuation coefficient (c) at nine wavelengths (10-nm FWHM) across the visible spectrum. Optical blanks for the ac-9 were regularly measured with ultrapure Millipore water treated with ultraviolet light to break down dissolved organic material. Calibration of the two optical channels remained within the manufacturer's specifications of $\pm 0.005\ m^{-1}$ throughout the cruise. Absorption and attenuation signals at 715 nm were corrected for temperature-dependent water absorption[8] and a scattering correction algorithm was applied to the absorption data[9]. The data were averaged over 1-m depth intervals, and the scattering coefficient (b) was obtained from the difference between absorption and attenuation. The ac-9 measures absorption and attenuation coefficients relative to pure water, a_{tot}–a_w and c_{tot}–c_w, where the subscripts tot and w refer to total and water coefficients, respectively. Total absorption coefficients were obtained by the addition of pure water values.[10]

Total backscattering, $b_{b\ tot}$, was measured at 470 and 676 nm with a Hydroscat-2 (HOBI Labs). Since calibration of this instrument is currently not possible in our laboratory, it was assumed that the manufacturer's calibration remained valid. Data were averaged into 1-m depth intervals. Because of current uncertainties over the most appropriate manner for correction of path-length effects, Hydroscat-2 data were left uncorrected.

C. Radiance Transfer Modeling

The Hydrolight (Sequoia Scientific) software package[11] was used to solve the radiative transfer equation for a range of coastal water conditions and a range of scattering phase functions and solar zenith angles. All simulations (bar one that was used to look at the effect of stratification) assumed homogeneous distributions of IOPs throughout the water column. For simulations in which the solar zenith angle or scattering phase function was varied, the input parameters were set to a chlorophyll concentration of 1 mg m^{-3}, a colored dissolved organic matter (CDOM) concentration corresponding to an absorption coefficient at 440 nm of 0.2 m^{-1} and a mineral concentration of 2 mg l^{-1}. Previous research suggests that these are reasonable values for the waters in which the AOP and the IOP model is tested in Section 4.[12] Absorption by phytoplankton and minerals was specified by use of the material-specific spectra provided with the software,[13] whereas scattering characteristics were defined by use of the near-surface Loisel–Morel parameters that are used to model scattering by use of a power-law function.[14] The CDOM absorption was modeled by

use of an exponential function with an exponent of 0.014. Water absorption values were provided by Pope and Fry.[10] Fournier–Forand[15] scattering phase functions were used for runs in which the backscattering ratio was varied. Fluorescence by phytoplankton and CDOM and Raman scattering effects were included in all the simulations. Surface solar irradiance was calculated by use of the RADTRAN model[16] with zero cloud input, and a wind speed of 5 ms^{-1} was used to simulate surface roughness. For runs to determine the effect of varying solar zenith angle and varying IOP composition, the average Petzold particle scattering phase function was selected. For runs that examine the effect of varying scattering phase function, the solar zenith angle was set to 30°. Simulations were carried out for solar zenith angles between 0° and 80°, for scattering phase functions with particulate backscattering ratios between 0.001 and 0.040, and for a range of IOPs that we varied by setting the chlorophyll concentration between 0.1 and 10 mg m^{-3} (a_{tot} varies between 0.24 and 1.09 m^{-1}, $b_{b\ tot}$ varies between 0.002 and 0.098 m^{-1}). All the simulations were performed to a depth of 10 m, which corresponds to between 2.9 and 17.7 optical depths depending on wavelength and input parameters. We examined the effect of a diffuse sky by carrying out a run with 100% cloud input. We examined stratification effects by running a simulation with two layers: (0–5 m) with chlorophyll $a = 1$ mg m^{-3}, and (5–10 m) with chlorophyll $a = 0.5$ mg m^{-3}.

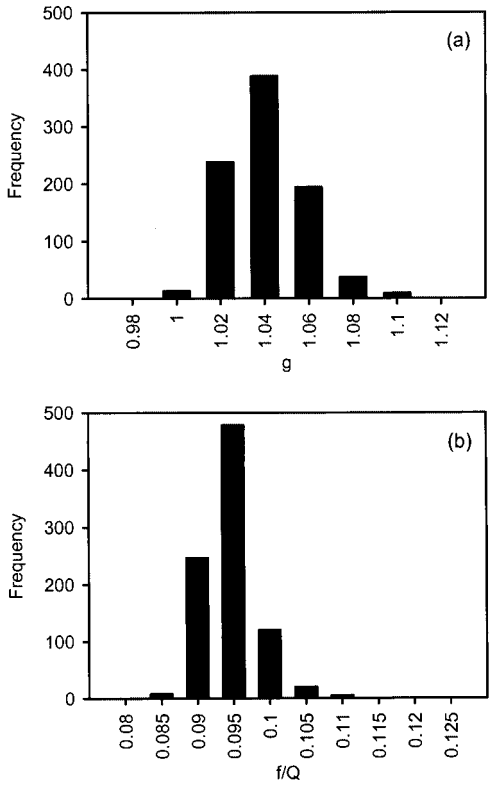

Fig. 2. Distributions of (a) the best-fit parameter g and (b) the ratio of f/Q. The data in these plots are for depths to 10 m, for five wavelengths in the blue-green part of the spectrum, and were derived from radiance transfer simulations that cover an extensive range of water column conditions.

4. Results

A. Variability of g and f/Q

The degree to which Eqs. (1) and (2) can be applied to depths greater than zero can be determined by examination of the results of the radiance transfer simulations described above. These simulations cover a wide range of IOPs and light field conditions. Figure 2 shows frequency distributions of g and f/Q for all the simulations described, for all depths down to 10 m, and for five wave bands in the blue-green part of the spectrum (412.5, 442.5, 490, 510, and 555 nm). The vast majority of observations of g were found between 1.02 and 1.06, with the greatest concentration in the 1.04 bin. This result is consistent with the value of 1.0395 found previously by Gordon[6] for surface data. The distribution of f/Q values is similar to that found by Morel and Gentili[7] for surface data. Their mean value of 0.0936 for f/Q lies at the center of the distribution obtained from radiance transfer simulations performed to depths down to 10 m. These results indicate that Eqs. (1) and (2) can be successfully applied below the surface. Table 1 gives mean values of both g and f/Q for each wavelength. These values are used in the analysis of the AOP and the IOP model throughout the rest of the paper.

B. Performance of the Apparent Optical Property and the Inherent Optical Property Model for Exact Values of $\mu_d(z)$

The first test of the AOP and the IOP model is to determine whether it is physically realistic. Equations (3) and (4) can be used to derive estimated values of absorption and backscattering (a_{est} and b_{best}) by use of values of K_d, R_L, and μ_d obtained from the radiance transfer simulations. These estimated values can then be compared with the values that were used as input for the radiance transfer simulations (a_{input} and $b_{b\ input}$). Figure 3 shows frequency distributions for the differences between input and estimated IOPs for this set of radiance transfer simulations. Maximum errors (of the order of 0.025 m^{-1} for a and 0.008 m^{-1} for b_b) occur for water columns with the highest levels of chlorophyll concentration (and therefore the highest values of

Table 1. Average Wavelength-Specific Values of g and f/Q from Radiance Transfer Simulations

λ (nm)	g	f/Q
412.5	1.0196	0.0896
442.5	1.0237	0.0909
490	1.0306	0.0933
510	1.0338	0.0934
555	1.0408	0.0940

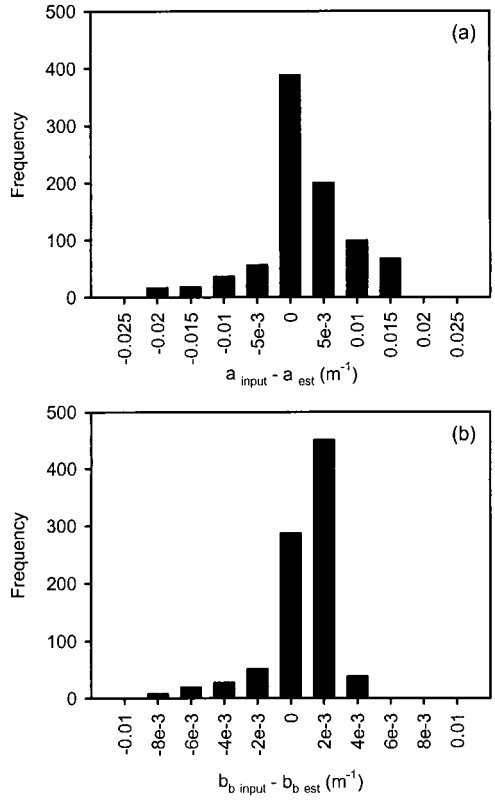

Fig. 3. Distributions of errors in estimations of (a) absorption and (b) backscattering obtained by use of Eqs. (3) and (4). Data were taken from radiance transfer simulations performed to a depth of 10 m for five wavelengths in the blue-green part of the spectrum. The mean cosine for downward irradiance is known exactly in this case.

absorption and scattering). However ~75% of the absorption estimates fit within the central three bins (i.e., within $\pm 0.0075\ m^{-1}$), and ~90% of backscattering estimates fit within the central three bins (i.e., within $\pm 0.003\ m^{-1}$). In percentage terms, the maximum errors are less than 4% for absorption and approximately 20% for backscattering. This seemingly large backscattering error is misleading, however, as it occurs for a very small particulate backscattering ratio (0.001) and represents an absolute error of less than $0.001\ m^{-1}$. For all simulations, wavelengths, and depths the average errors for absorption and backscattering estimates are ~1% and ~3%, respectively. The AOP and the IOP relationships modeled by Eqs. (3) and (4) are therefore physically realistic, and, when μ_d is known, these equations provide useful estimates of a and b_b for nearly all simulated water columns.

C. Performance of the Model for Approximate Values of $\mu_d(z)$

As discussed previously, the E_d–L_u radiometer configuration does not provide an explicit value of $\mu_d(z)$. Therefore, to apply the AOP and the IOP model to data restricted to the L_u–E_d configuration, it becomes necessary to use approximate values of $\mu_d(z)$. Each of the approximations discussed previously was applied to the set of radiance transfer simulations and the effect of each approximation on the accuracy of estimations of a and b_b was observed. Table 2 provides a summary of the results of this analysis. The best-performing approximation is $K_d(z)\mu_d(z) \approx K_d(0)\mu_d(0)$, which provides results that are close to those obtained with exact values of $K_d(z)$ and $\mu_d(z)$. Unfortunately, this approximation is difficult to put into practice with SPMR data because the algorithm used to calculate $K_d(z)$ averages the data over several meters: values of $K_d(z)$ are generally available from 3 m downward when the E_d bin size is 1 m. The effect of using $K_d(3)$ instead of $K_d(0)$ is to make the average error in both estimates similar to those found by use of $\mu_d(z) = 0.75$ and $\mu_d(z) = \mu_d(0)$. There is therefore little to separate the three approximations for $K_d(z)\mu_d(z)$ in practice.

Table 2. Errors in IOP Retrieval Associated with Different Approximations for $K_d(z)\mu_d(z)$

Approximation	Average Percentage Error	
	a	b_b
$K_d(z)\mu_d(z)$	1.09	3.11
$K_d(0)\mu_d(0)$	2.26	3.38
$K_d(3)\mu_d(0)$	13.56	13.51
$K_d(z)\mu_d(0)$	13.10	13.64
$K_d(z)0.75$	13.97	14.16

D. Estimation of Inherent Optical Properties from *in situ* Measurements

A total of 20 stations were occupied in the Clyde Sea between 10 and 27 April 2001. Profiles of IOPs and AOPs were taken at a variety of times of day, with solar zenith angles in air that varied between 42.5° and 55°. Equations (3) and (4) were used to generate a set of estimated absorption and backscattering coefficients that could be compared with ac-9 and Hydroscat-2 measurements made *in situ*. We determined station by station the maximum depth for which data were taken for this analysis by selecting the depth at which the SPMR signal approached its dark value in the 412-nm wave band. For this set of data this depth occurred between 8 and 25 m. It was found that the best match between estimated and measured IOPs was obtained by use of the $K_d(z)\mu_d(z) = K_d(z)\ \mu_d(0)$ approximation. Figure 4(a) shows absorption estimated by use of this approximation versus *in situ* measurements of absorption for five wavelengths in the blue-green part of the spectrum where there is a good wavelength match (within 3 nm) between the ac-9 and the SPMR. Clearly there is a strong correlation ($r^2 = 0.95$) between measured and estimated absorption coefficients, and the 1:1 line passes through the data set. Figure 4(b) shows estimates of backscattering based on SPMR measurements at 490 nm plotted against Hydroscat-2 *in situ* backscattering measurements at 470 nm. Despite

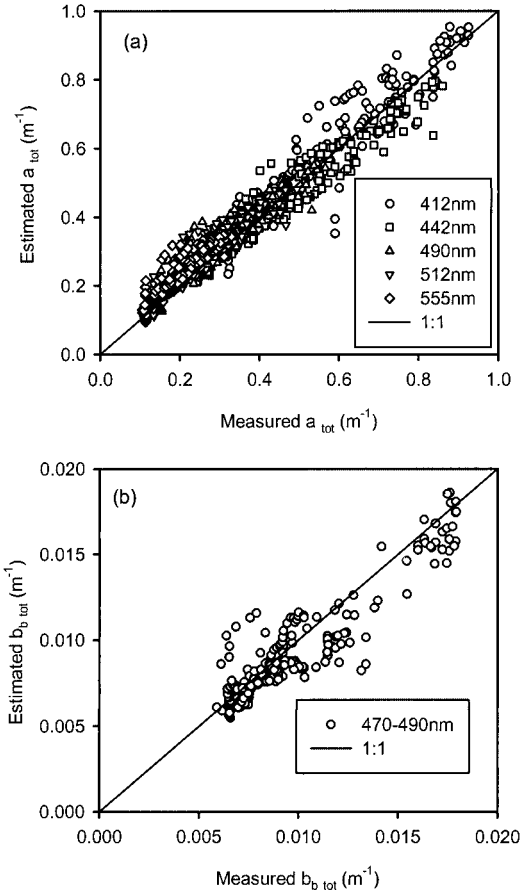

Fig. 4. IOPs estimated by use of Eqs. (3) and (4) plotted against independent *in situ* measurements taken of (a) absorption and (b) backscattering off the west coast of Scotland. Estimates are based on the approximation $K_d(z)\mu_d(z) = K_d(z)\mu_d(0)$.

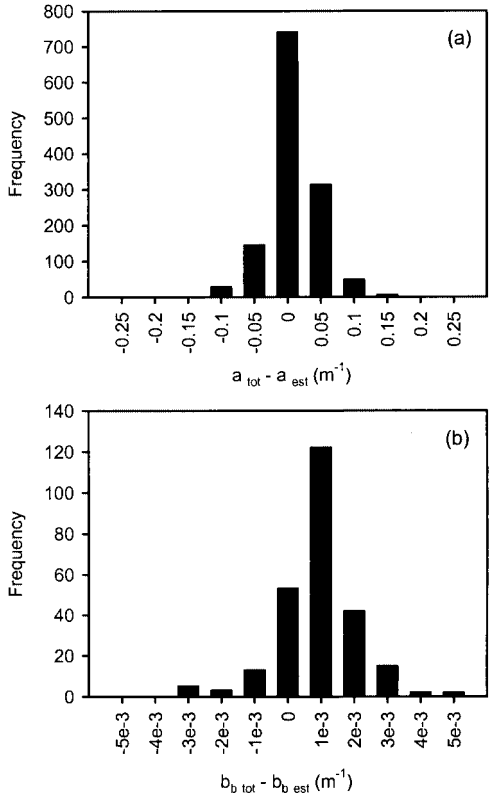

Fig. 5. Distributions of the error in estimation of (a) absorption and (b) backscattering for field data from the west coast of Scotland. These estimates are based on the approximation $K_d(z)\mu_d(z) = K_d(z)\mu_d(0)$.

the wavelength mismatch between the Hydroscat-2 and the SPMR, this plot shows a remarkable degree of correlation ($r^2 = 0.85$).

Figure 5(a) shows that the distribution of errors in the estimated absorption coefficients is centered on zero. Just less than 60% of points lie in the central bin (± 0.025 m^{-1}) and more than 90% of points lie within the central three bins (± 0.075 m^{-1}). This translates into an average percentage error of approximately 10%, which is of a similar magnitude to the error observed by use of the $K_d(z)\mu_d(z) = K_d(z)\mu_d(0)$ approximation on the results of the radiance transfer simulations. The magnitude of the absolute error appears to be independent of wavelength and has an average value of ~ 0.03 m^{-1}. An increase in the percentage error from blue-to-green wavelengths is due primarily to the absorption in the green being significantly lower than in the blue for these waters.

The distribution of errors in the estimate of the backscattering coefficient shown in Fig. 5(b) shows a slight positive bias (0.001 m^{-1}). This could be attributable to a small instrument offset in the Hydroscat-2, or it might be a result of the wavelength mismatch between the SPMR and the Hydroscat-2. If the distribution is shifted by an offset of 0.001, then approximately 50% of points fall within the central bin (± 0.0005 m^{-1}) and 85% of points lie within the central three bins (± 0.0015 m^{-1}). Without application of any offset correction, the average percentage error is less than 10% and corresponds to an average absolute error of 0.0009 m^{-1}. This level of error is similar to that observed when the AOP and the IOP model was applied to the results of the radiance transfer simulations and the $K_d(z)\mu_d(z) = K_d(z)\mu_d(0)$ approximation was used.

5. Discussion

A simple set of equations that relates AOPs and IOPs has been developed and tested using radiance transfer modeling and *in situ* measurements. These equations can be used to retrieve absorption and backscattering coefficients from diffuse attenuation coefficients, radiance reflectances, and mean cosines for downward irradiances. If all three AOPs required for the model are known, it is possible to estimate both absorption and backscattering with an average error of just 1% and 3%, respectively. Furthermore, it is possible for one to estimate a and b_b (with a typical accuracy of $\sim 10\%$) from just two radiometric measurements, E_d and L_u, by setting the mean cosine for downward irradiance equal to its value just beneath the surface, $\mu_d(0)$. E_d and L_u are

already commonly measured by ocean color laboratories and are more widely available than the three parameters (E_d, L_u, and E_u) used in an earlier study by Stramska *et al*.[4]

Equations (3) and (4) have several useful applications. When concurrent IOP and AOP data sets are available, they can be used to validate the quality of the data set. They can be used with time series measurements of L_u and E_d from arrays of vertically displaced radiometers to generate estimated time series of a and b_b. They might also be of interest to those engaged in ground-truthing exercises for ocean color satellite imagery as both R_L and K_d can be retrieved to some extent from remote-sensing data.[7,17,18]

Another application arises from the fact that submersible hyperspectral scalar irradiance sensors have recently become commercially available. Since $\mu_d = E_d/E_{od}$, where E_{od} is the downward scalar irradiance, it will be possible to measure $\mu_d(z)$ *in situ*. This raises the prospect of using a combination of hyperspectral radiance, irradiance, and scalar irradiance sensors to provide high resolution *in situ* IOPs that are currently not measurable by any other means. This combination of sensors would be of particular use for combined studies of primary productivity and remote sensing.

The retrieval technique has been tested in coastal case II waters off the west coast of Scotland, but analysis of radiative transfer simulations suggests that it should be equally successful for a fairly wide range of conditions. Further research in different water types and latitudes is required to establish how widely it can be applied, but suitable data sets probably exist in the archives of most ocean color laboratories.

References

1. Z. P. Lee, K. L. Carder, T. G. Peacock, C. O. Davis, and J. L. Mueller, "Method to derive ocean absorption coefficients from remote-sensing reflectance," Appl. Opt. **35,** 453–462 (1996).
2. R. A. Leathers and N. J. McCormick, "Ocean inherent optical property estimation from irradiances," Appl. Opt. **36,** 8685–8698 (1997).
3. R. A. Leathers, C. S. Roesler, and N. J. McCormick, "Ocean inherent optical property determination from in-water light field measurements," Appl. Opt. **38,** 5096–5103 (1999).
4. M. Stramska, D. Stramski, B. G. Mitchell, and C. D. Mobley, "Estimation of the absorption and backscattering coefficients from in-water radiometric measurements," Limnol. Oceanogr. **45,** 628–641 (2000).
5. H. Loisel and D. Stramski, "Estimation of the inherent optical properties of natural waters from the irradiance attenuation coefficient and reflectance in the presence of Raman scattering," Appl. Opt. **39,** 3001–3011 (2000).
6. H. R. Gordon, "Can the Lambert–Beer law be applied to the diffuse attenuation coefficient of ocean water?," Limnol. Oceanogr. **34,** 1389–1409 (1989).
7. A. Morel and B. Gentili, "Diffuse reflectance of oceanic waters. II. Bidirectional aspects," Appl. Opt. **32,** 6864–6879 (1993).
8. W. S. Pegau and J. R. V. Zaneveld, "Temperature-dependent absorption of water in the red and near-infrared portions of the spectrum," Limnol. Oceanogr. **38,** 188–192 (1993).
9. J. R. V. Zaneveld, J. C. Kitchen, and C. C. Moore, "Scattering error correction of reflection-tube absorption meters," in *Ocean Optics XII,* J. S. Jaffe, ed., Proc. SPIE **2258,** 44–55 (1994).
10. R. M. Pope and E. S. Fry, "Absorption spectrum (380–700 nm) of pure water. II. Integrating cavity measurements," Appl. Opt. **36,** 8710–8723 (1997).
11. C. D. Mobley, *Light and Water: Radiative Transfer in Natural Waters* (Academic, San Diego, Calif., 1994).
12. D. McKee, A. Cunningham, J. Slater, K. J. Jones, and C. R. Griffiths, "Inherent and apparent optical properties in coastal waters: a study of the Clyde Sea in early summer," Estuarine Coastal Shelf Sci. (to be published).
13. L. Prieur and S. Sathyendranath, "An optical classification of coastal and oceanic waters based on the specific spectral absorption curves of phytoplankton pigments, dissolved organic matter, and other particulate materials," Limnol. Oceanogr. **26,** 671–689 (1981).
14. H. Loisel and A. Morel, "Light scattering and chlorophyll concentration in Case 1 waters: a reexamination," Limnol. Oceanogr. **43,** 847–858 (1998).
15. G. R. Fournier and J. L. Forand, "Analytic phase function for ocean water," in *Ocean Optics XII,* J. S. Jaffe, ed., Proc. SPIE **2258,** 194–201 (1994).
16. W. W. Gregg and K. L. Carder, "A simple spectral solar irradiance model for cloudless maritime atmospheres," Limnol. Oceanogr. **35,** 1657–1675 (1990).
17. R. W. Austin and T. J. Petzold, "The determination of the diffuse attenuation coefficient of seawater using the Coastal Zone Color Scanner," in *Oceanography from Space*, J. F. R. Gower, ed. (Plenum, New York, 1981), pp. 239–256.
18. A. Morel and B. Gentili, "Diffuse reflectance of oceanic waters. III. Implication of bidirectionality for the remote sensing problem," Appl. Opt. **35,** 4850–4862 (1996).